20th Australasian Fluid Mechanics Conference
Perth, Australia
5-8 December 2016

# Effects of Forces Induced by Steady Streaming Flows on Rigid Oscillating Spheres

**J. Jalal[1], J. S. Leontini[1], D. Fabre[2], and R. Manasseh[1]**

[1]Faculty of Science, Engineering and Technology
Swinburne University of Technology, Victoria 3122, Australia

[2]Université de Toulouse; INPT, UPS; IMFT (Institut de Mécanique des Fluides de Toulouse);
Allée Camille Soula, F-31400 Toulouse, France.

## Abstract

A numerical method based on a perturbation approach is used to compute the microstreaming flow fields around a pair of spheres, along with the forces experienced on the spheres positioned at any arbitrary distance apart. The perturbation approach is first validated against a DNS and the literature. The aim is to determine the role of steady streaming causing particles to attract each other.

## Introduction

Acoustics has recently been used to separate cream from milk [9]. When ultrasound is applied, a standing wave is formed in the fluid, which causes particles to collect at nodal or antinodal regions ([4], [6], [13]). In the case of milk, these particles are micron-sized, spherical, Milk Fat Globules (MFGs) that rise and separate as cream. The phenomenon of oscillating spheres travelling from nodes to antinodes in an acoustic field caused by the Direct Radiation Force (DRF) ([6], [13]) is well known to the responsible for this aggregation. It is also possible that the phenomenon of steady streaming around the oscillating spheres [12] also affects the aggregation. There is an extensive literature on DRF and their effects for spherical particles, but less attention is paid to miscrostreaming effects. The streaming flow around a sphere in a sound field was first analysed by C. A. Lane in 1955. Lane recognised that there are inner vortices in the boundary layer around a spherical particle that would drive outer vortices much bigger in size than the particle itself [8]. Longuet-Higgins [11] later computed steady streaming around spherical oscillating particles, but he did not take into account the forces involved.

The focus of this work is to find the role of steady streaming in beneficially bringing particles together or detrimentally preventing the process, through a study of forces involved. In particular, we are interested in the threshold of frequency at which this process occurs. A numerical method based on perturbation approach is used to calculate forces exerted on two spheres. The method is first validated by a Direct Numerical Simulation (DNS) for streaming around a single sphere.

## Numerical Method

We have used a perturbation method to calculate forces exerted by two spheres on each other solving the Weakly Non-Linear equations (WNL) in FreeFem++ [5]. In order to validate the perturbation method, we have first applied a full DNS for a single sphere of unit diameter $D$. An unbounded, incompressible fluid is assumed to be oscillating vertically with an amplitude $A$ and frequency $\omega$. For the case of two spheres, two stationary equisized spheres of unit diameter are fixed at a position with distance $L$ apart and angle $\theta$ between their centers. A Cartesian $(x,y,z)$ frame of reference is used together with a cylindrical $(r,\varphi,z)$ frame. When $\theta = 0°$, the spheres are placed parallel to the axis of imposed oscillation, in an axial configuration. Similarly at $\theta = 90°$, the spheres are positioned perpendicular to the axis of imposed oscillation, in a lateral configuration.

We defined the non-dimensional parameters, $\varepsilon = A/D$, described in the literature as inverse Strouhal number, and Reynolds number $Re = A\omega D/\nu$, where $D$ is the diameter, $A$ is the amplitude and $\omega$ is the frequency of the oscillating flow, and $\nu$ is the kinematic viscosity. For the WNL approach applied for two spheres, a ratio of $Re$ and $\varepsilon$ is introduced as $\Omega = \omega R^2/\nu$, where $R = D/2$. In this case, we assumed that $\varepsilon \to 0$.

## Validation for the Case of a Single Sphere

The DNS applied a spectral element method approach to solve the problem [10]. The numerical scheme integrated Navier-Stokes equations with respect to time using a mixed explicit-implicit time-splitting scheme based on backwards differentiation. A second order time variant of the method was employed for all calculations. The Gauss-Lobatto-Legendre quadrature was used for integration. Oscillating boundary conditions were applied on left and right sides for incoming and outgoing flow, with pressure gradient $dp/dx = 0$. At the top boundary, the flow was parallel ($v = 0$), with zero-stress ($du/dy = 0$), and the pressure gradient $dp/dy = 0$. In addition to a no-slip, the normal gradient of the pressure $dp/dn = 0$ at the surface of the sphere. We assumed an axi-symmetry over the axis of the oscillating flow. We used the same mesh design as used by Blackburn [3]. The rectangular mesh, with a full extent of domain = $100D$, is designed in a way so that it is refined enough to capture the micro-streaming effects near the boundary of the sphere. The outer mesh is kept coarse to save computational time.

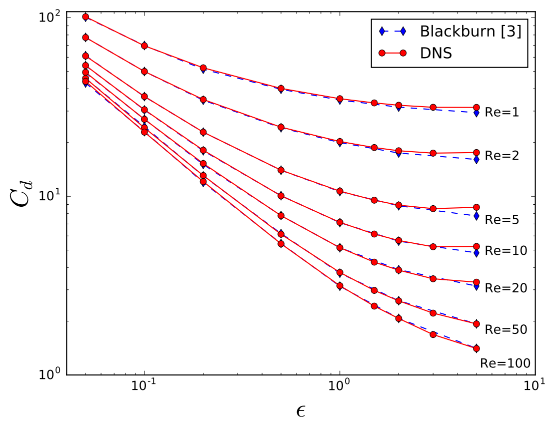


Figure 1: Comparison of peak coefficients of drag, $C_d$, for a stationary sphere in an oscillating flow.

### Validation of DNS

We have measured peak coefficients of a drag force for a stationary sphere in oscillatory flow as a function of $Re$, using DNS shown in Figure 1. It matches well with Blackburn

[3], that in turn matches with Basset's analytical solution [2] for amplitudes $\leq 1$. For MFGs in ultrasound, $\varepsilon$ is typically $O(10^{-2} - 10^{-1})$, implying the WNL approach, which assumes $\varepsilon \to 0$ can be validated against the DNS.

For a further validation of DNS, we made a comparison of inner vortical sizes with Blackburn [3] and Alassar [1], by measuring lengths of stagnation points on the axis of oscillation and they agree well.

### Validation of Results from WNL by DNS

We have made a qualitative and quantitative comparison of the size of the inner vortices measured using DNS and WNL. For a qualitative comparison (Figure 2), we compare the streaming flows around the spheres, which agrees with the theoretical predictions of Lane [8] as well. We quantitatively measured the

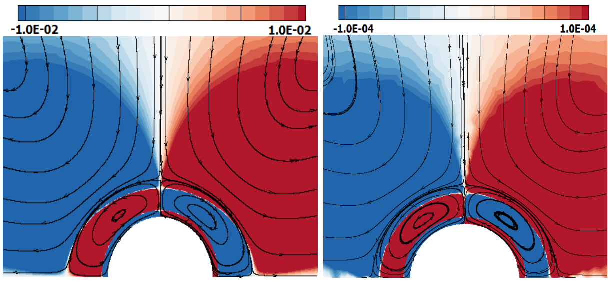


Figure 2: Flows generated using: (left) DNS for $Re = 100$, when $\varepsilon = 0.25$, and (right) WNL for $\Omega = 100$. The colour contour represents vorticity.

size of the vortices in a non-dimensional term, $r_{cross}$, by measuring the length of stagnation points in the direction parallel to the imposed oscillation (Figure 3).

### Validation and Results for the Case of Two Spheres

We have first validated our results with Klotsa et al. [7] to measure interaction force, $F_r$, as a function of the distance between the center of two spheres, $r$, after non-dimensionalizing the parameters. $F_r$ has been computed for a pair of spheres for experiments in [7], vibrated at 50 Hz with relative amplitude of the spheres with respect to the cell $A_r = 0.28$ mm in a fluid of viscosity $4.5 \times 10^{-6} m^2 s^{-1}$. These values are used to achieve the curve in Figure 4 where the corresponding $Re \approx 20$. When converted to our parameters, this gives a value of $\Omega = 17.85$. This value is quite accurate given that the setup used by Klotsa et al. [7] is only a small cell of domain extent of $6R$, including boundary effects on the spheres, whereas in our simulations the spheres are assumed to be immersed in the liquid where extent of the domain is $100D$.

We presented the effect of mean forces due to steady streaming for changing distance between two spheres for low to high frequencies i.e. $1 \leq \Omega \leq 100$. Mesh dependence has been checked over various combinations of domain sizes and mesh densities, comprising of a refined inner circular region close to the sphere(s), and a coarser outer one further away. We found that results vary only $< 1\%$ across all the meshes, when measuring forces for all values of $\Omega$, shown in Figure 6. Figure 7 shows streaming flows around two spheres in three different configurations, discussed below, for different values of $\Omega$. Since the oscillation is imposed vertically, in these cases, the streamlines going inwards towards the spheres in the vertical direction will suggest an attraction between them. Similarly, streamlines going outwards in the vertical direction will suggest a repulsion.

When the spheres are in a lateral configuration, the mean force in the axial direction is attractive for high frequencies and repulsive for low frequencies (Figure 5, Figure 6(a)). For intermediate values of $\Omega$, the mean force exerted on the spheres reduces rigorously to zero so the spheres stay at an equilibrium position. In this configuration, there are only four large inner vortices at $\Omega = 1$, that will reduce in size as the frequency increases (Figure 7(a)). At around $\Omega = 8$, another pair of vortices appears for each sphere in between the spheres. As the frequency further increases, the previous larger inner vortices adjust their size with the newly formed small vortices, until they are of the same size. Meanwhile, the outer vortices are now overpowering the inner vortices at $\Omega = 100$.

In the axial configuration, the mean force in the axial direction shows an opposite trend to that of the transverse configuration (Figure 6(b)). It is attractive for low frequencies and repulsive for high frequencies. For intermediate values of $\Omega$, the mean force is attractive when the spheres are at a small distance apart, but is repulsive for large distances. This points out existence of an unstable equilibrium position. At $\Omega = 1$, the eight inner vortices are very strong, comprising of four small ones that are in between the spheres and four large ones around them (Figure 7(b)). As the frequency increases, the size of these inner vortices starts to decrease. The outer vortices start to increase in size correspondingly. This continues until the inner vortices are confined close to the boundary of each sphere. The outer vortices keep growing, until at around $\Omega = 30$, there is a change

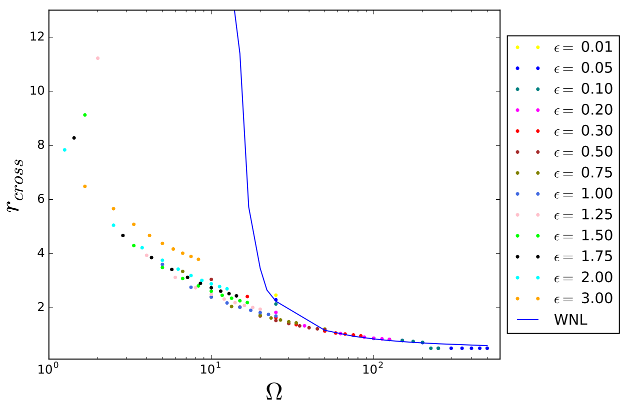


Figure 3: Comparison of size of the inner vortices, $r_{cross}$, in non-dimensional terms, when the oscillation of the sphere is parallel to that of the imposed oscillation, measured by DNS and WNL (using FreeFem++).

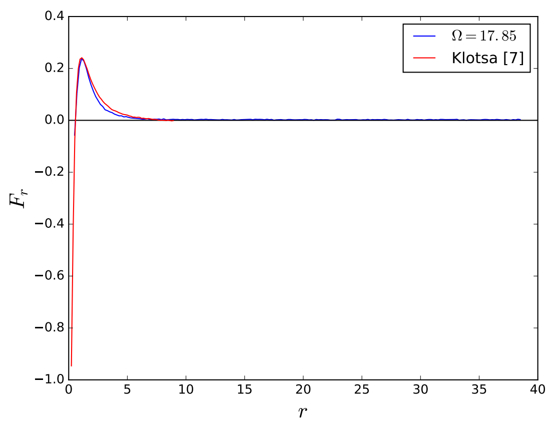


Figure 4: The curve for $F_r$, as a function of space between the spheres, $r$, using simulation by [7]. We match this curve using our simulation when $\Omega = 17.85$.

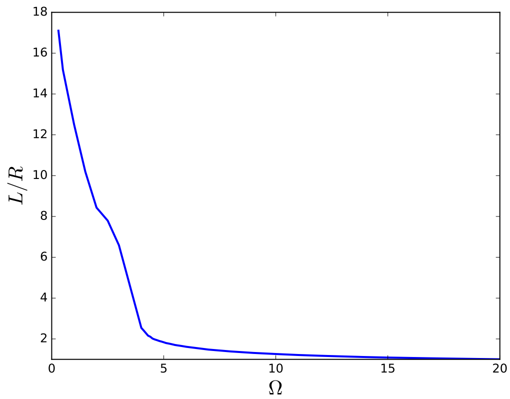


Figure 5: Distance between the center of the spheres, $L/R$, as a function of frequency, $\Omega$, in a lateral configuration.

in topology. Another set of vortices is quite noticeable around the two spheres. There are now twelve vortices close to spheres in addition to four outer ones at $\Omega = 100$.

The oblique configuration refers to spheres positioned at $\theta = 45°$, shown in Figure 6(c). There is a similar trend for the case of spheres in oblique configuration to that of lateral configuration. Four large inner vortices are accompanied by another one in between the spheres at lower frequencies (Figure 7(c)). As the frequency is increased, another pair of vortices starts to appear perpendicular to the axis of oscillation at around $\Omega = 8$. The shared central vortex splits into two at $\Omega = 30$, that get noticeable after this point and contribute to the inner vortices present in between the spheres. All these vortices keep shrinking until they are all confined closed to the boundary of the spheres by the now larger outer vortices at $\Omega = 100$, in addition to another shared vortex between the spheres.

### Conclusions

We have validated a new computational method based on a perturbation method, to study forces and streaming flows around one and two spheres in an oscillating flow. It is much quicker and less expensive than the DNS, especially for the case when flows around two spheres are considered. We have discussed regimes where two spheres can attract or repel each other in three different configurations for different frequencies. This work can be can easily extended for spheres of different radii, and for ellipsoids and cylinders.


### Acknowledgments

This work was funded by the Australian Research Council (ARC LP110200499 and ARC DP150103177) and the Geoffrey Gardiner Dairy Foundation.


### References


[1] Alassar, R. S., Acoustic streaming on spheres, *International Journal of Non-Linear Mechanics*, **43**, 2008, 892–897.

[2] Basset, A. B., *A treastise on hydrodynamics*, volume 2, Deighton, Bell and Co., Cambridge, England, 1888.

[3] Blackburn, H. M., Mass and momentum transport from a sphere in steady and oscillatory flows, *Physics of Fluids*, **14**, 2002, 3997.

[4] Doinikov, A., Acoustic radiation forces : classical theory and recent advances, *Recent Res Devel Acoustics*, **661**, 2003, 39–67.


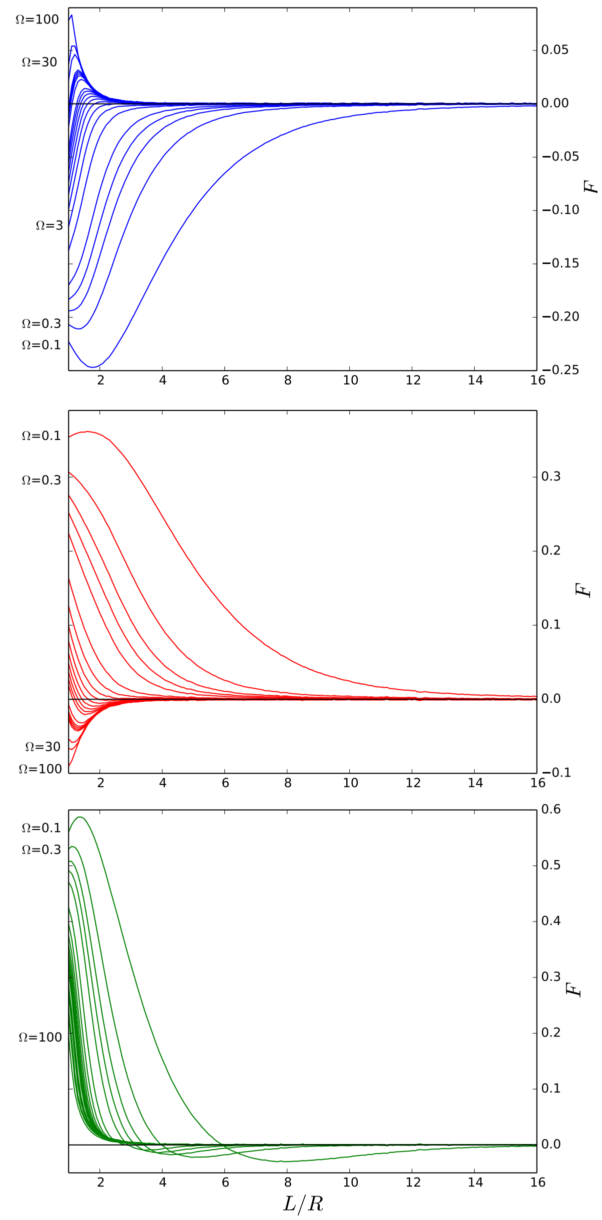


Figure 6: Non-dimensional Force, $F$, exerted on spheres by steady streaming as a function of distance $L/R$ in between them for different values of $\Omega$ in the: (a) Lateral configuration, (b) Axial configuration, and (c) Oblique configuration.


[5] Fabre, D., Jalal, J., Leontini, J. S. and Manasseh, R., Acoustic streaming and its induced forces between two fixed spheres, *Journal of Fluid Mechanics (Submitted)*.

[6] King, L. V., On the Acoustic Radiation Pressure on Spheres, *Proceedings of the Royal Society A: Mathematical, Physical and Engineering Sciences*, **147**, 1934, 212–240.

[7] Klotsa, D., Swift, M., Bowley, R. and King, P., Interaction of spheres in oscillatory fluid flows, *Physical Review E*, **76**, 2007, 056314.

[8] Lane, C. A., Acoustical Streaming in the Vicinity of a Sphere, *The Journal of the Acoustical Society of America*, **27**, 1955, 1082.

[9] Leong, T., Johansson, L., Mawson, R., McArthur, S. L., Manasseh, R. and Juliano, P., Ultrasonically enhanced

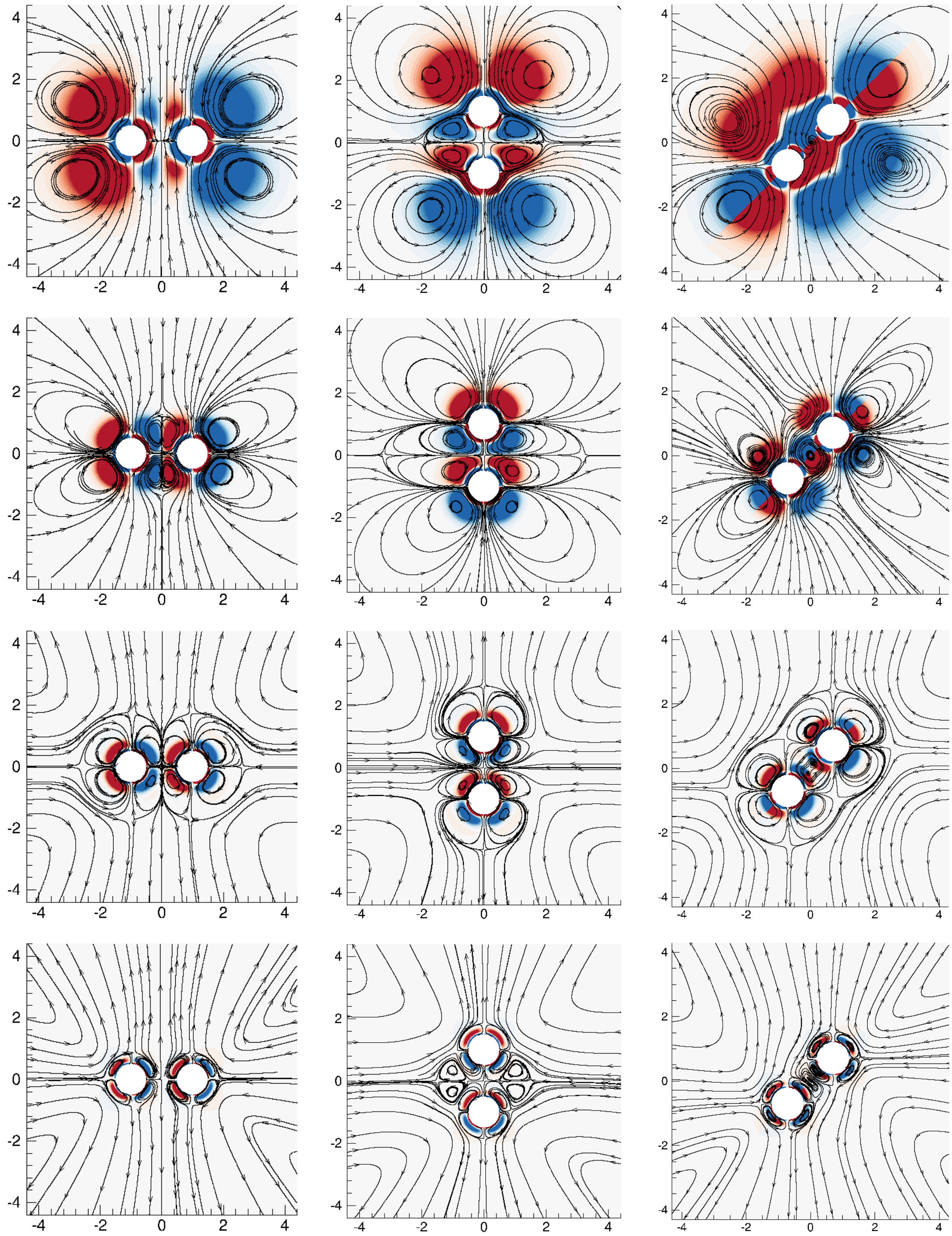

a) Lateral configuration b) Axial configuration c) Oblique configuration

Figure 7: Steady streaming around two spheres in a) lateral, b) axial, and c) oblique configuration for $\Omega = 1$, $\Omega = 8$, $\Omega = 30$, and $\Omega = 100$, in each row respectively, from top to bottom, when $L/R$=2. The colours represent vorticity contours between $-0.01$ to 0.01.


fractionation of milk fat in a litre-scale prototype vessel., *Ultrasonics sonochemistry*, **28**, 2016, 118–29.

[10] Leontini, J. S., Thompson, M. C. and Hourigan, K., Three-dimensional transition in the wake of a transversely oscillating cylinder, *Journal of Fluid Mechanics*, **577**, 2007, 79–104.

[11] Longuet-Higgins, M. S., Viscous streaming from an oscillating spherical bubble, *Proceedings of the Royal Society A: Mathematical, Physical and Engineering Sciences*, **454**, 1998, 725–742.

[12] Riley, N., Steady Streaming, *Annual Review of Fluid Mechanics*, **33**, 2001, 43–65.

[13] Yosioka, K. and Kawasima, Y., Acoustic Radiation Pressure on a Compressive Sphere, *Acustica*, **5**, 1955, 167–173.